DMD Fast Forward. Published on July 14, 2020 as DOI: 10.1124/dmd.120.090498

Quantification of the Impact of Partition Coefficient Prediction Methods on PBPK Model Output Using a Standardized Tissue Composition

Kiersten Utsey[1,2], Madeleine S Gastonguay[1,3], Sean Russell[1,4], Reed Freling[1,5], Matthew M Riggs[1], Ahmed Elmokadem[1]

[1]Metrum Research Group, Tariffville, CT, USA; [2]University of Utah, Salt Lake City, UT, USA; [3]University of Connecticut, Storrs, CT, USA; [4]University of Michigan, Ann Arbor, MI, USA; [5]Cornell University, Ithaca, NY, USA

Running Title: Impact of partition coefficient methods on PBPK modeling

Corresponding author:

Ahmed Elmokadem

2 Tunxis Rd, Tariffville, CT, USA

Fax: 8607606014

Phone: 8608404480

email: ahmede@metrumrg.com

Number of text pages: 31

Number of tables: 2

Number of figures: 9

Number of references: 34

Number of words in the *Abstract*: 224

Number of words in the *Introduction*: 703

Number of words in the *Discussion*: 1072

Abbreviations:

Absorption, distribution, metabolism and excretion (ADME); albumin ratio (AR); Berezhkovskiy prediction method (Berez); unbound fraction in plasma (fu_p); lipophilicity (log*P*); lipoprotein ratio (LR); tissue:plasma partition coefficients (K_p); Pearson correlation coefficient (PCC); default PK-Sim prediction method (PK-Sim); Poulin and Theil prediction method (PT); red blood cells (RBCs); root mean square error (RMSE); Rodgers and Rowland prediction method (RR);

Schmitt prediction method (Schmitt); Pharmacokinetic (PK); Physiologically-based pharmacokinetic (PBPK).

Abstract

Tissue:plasma partition coefficients are key parameters in physiologically-based pharmacokinetic (PBPK) models, yet the coefficients are challenging to measure *in vivo*. Several mechanistic-based equations have been developed to predict partition coefficients using tissue composition information and the compound's physicochemical properties, but it is not clear which, if any, of the methods is most appropriate under given circumstances. Complicating the evaluation, each prediction method was developed, and is typically employed, using a different set of tissue composition information; thereby making a controlled comparison impossible. This study proposed a standardized tissue composition for humans that can be used as a common input for each of the five frequently used prediction methods. These methods were implemented in R and were used to predict partition coefficients for 11 drugs, classified as strong bases, weak bases, acids, neutrals, and zwitterions. PBPK models developed in R (*mrgsolve*) for each drug and each set of partition coefficient predictions were compared to respective observed plasma concentration data. Percent RMSE and half-life percent error were used to evaluate the accuracy of the PBPK model predictions using each partition coefficient method as summarized by strong bases, weak bases, acids, neutrals, and zwitterions characterization. The analysis indicated that no partition coefficient method consistently yielded the most accurate PBPK model predictions. As such, PBPK model predictions using all partition coefficient methods should be considered during drug development.

Significance Statement

Several mechanistic-based methods exist to predict tissue:plasma partition coefficients critical to PBPK modeling. Controlled comparisons are confounded by the use of different tissue composition values for each method; a standardized tissue composition was proposed. Resulting assessments indicated that no method was consistently superior; therefore, sensitivity of PBPK predictions to each method may be warranted prior to model optimization.

Introduction

Physiologically-based pharmacokinetic (PBPK) models predict the absorption, distribution, metabolism, and excretion (ADME) properties of a drug at physiologically-relevant (e.g., tissue and organ) scales. Since PBPK models are based on first principles, they can be used to make pharmacokinetic (PK) predictions for the drug of interest prior to conducting clinical trials. Common applications include first-in-human, environmental toxicology, or rare disease populations studies (Jones and Rowland-Yeo, 2013). These models combine physiological data with drug physicochemical properties to parameterize ordinary differential equations that represent the ADME processes. Among the drug-related parameters are the tissue:plasma partition coefficients (K_p). *In vivo* experiments that measure tissue and plasma drug concentrations over time and at steady-state can determine K_p values, however these experiments are expensive and time-consuming (Jones and Rowland-Yeo, 2013). As such, these experiments cannot be used for routine data collection in drug discovery. Several *in silico* methods have been developed to predict K_p values from more easily obtained *in vitro* data. Using a combination of tissue composition information and the compound's physicochemical characteristics, like lipophilicity (log*P*) and the unbound fraction in plasma (fu_p), these methods account for the distribution of the drug between water and drug-binding components, including proteins, lipids, and phospholipids.

Each method assumes that drugs are distributed homogeneously into plasma and each tissue via passive diffusion. They also account for non-specific binding to tissue components, including lipids, phospholipids, and proteins. Although each prediction method is based on the same general mechanisms, the methods differ in complexity and the type of experimental information required. Poulin and Theil (PT) initially proposed a tissue:plasma partition coefficient prediction method that accounts for dissolution into water and non-specific binding to neutral lipids and phospholipids (Poulin and Theil, 2002). Lipophilicity was estimated by the

octanol:water partition coefficient for non-adipose tissue and the oil:water partition coefficient for adipose. Berezhkovskiy (Berez) modified the PT method and assumed only drugs in the water fraction bind to tissues (Poulin and Theil, 2002; Berezhkovskiy, 2004). Rodgers and Rowland (RR) extended Poulin and Theil's method to consider the impact of drug ionization on partitioning (Rodgers *et al.*, 2005; Rodgers and Rowland, 2006). In particular, the new equations in RR accounted for the dissolution of the drug into water, partitioning of unionized drugs into neutral lipids and phospholipids, electrostatic interactions between moderate-to-strong bases and acidic phospholipids, and interactions between extracellular proteins and weak bases, acids, neutrals, and zwitterions. Schmitt considered a universal method that separated tissues into water, neutral lipids, neutral and acidic phospholipids, and protein fractions (Schmitt, 2008). Unlike the previous methods, Schmitt accounted for electrostatic interactions between positively charged molecules and acidic phospholipids. Willmann and co-workers (PK-Sim) proposed a method that considered partitioning into lipids, proteins, and water, and used membrane affinity as a lipophilicity measure (Willmann *et al.*, 2005). Other empirical methods requiring *in vivo* data, such as the volume of distribution or the partition coefficient for one tissue, have been proposed (Arundel, 1997; Jansson *et al.*, 2008; Poulin and Theil, 2009). This study considers only commonly used, mechanistic-based methods that require only *in vitro* data.

Given the wide variability in K_p predictions between these different *in silico* methods, Graham and co-workers were motivated to compare the predictive performance between three mechanistic methods (PT, Berez, and RR) and three empirical methods to determine the most accurate method for rat partition coefficients (Graham *et al.*, 2012). The study found that among predictions made by the mechanistic-based methods and empirical methods, the predictions made by RR were most accurate, in comparison to experimentally determined K_p values (Graham *et al.*, 2012). That study only considered K_p predictions for rat tissues, however, and was not extended to the human physiology that is often markedly different than rats (Graham *et*

al., 2012). Additionally, the rat tissue composition used was the one reported by Rodgers and Rowland, which might have led to some bias towards that method. Given the limited availability of experimentally measured human partition coefficients, this study described herein uses a different strategy to compare partition coefficient predictions from different methods.

The goal of the current study was to investigate the impact of five commonly used tissue:plasma partition coefficient prediction methods (PT, Berez, RR, Schmitt, and PK-Sim) on PBPK model predictions based on a standardized human physiology and the physicochemical properties of 11 distinct drugs.

Methods

Overview

The workflow for the analyses described herein followed a five-step approach (Figure 1). The first two steps involved the recapitulation of the mathematical expressions used in the published K_p estimation equations into R functions with subsequent reviews to ensure their proper translation and application of these estimation methods. The third and fourth steps involved the development and qualification of a standardized tissue composition database to act as a control set in the underlying PBPK model while investigating the impact of the different K_p estimation methods. The final stage integrated the previous steps to then evaluate each K_p estimation method using drugs that were representative of a range of physicochemical properties (strong base, weak base, acid, neutral, and zwitterion). Additional methodology for each step is provided in the sections below.

Tissue:plasma partition coefficient calculation methods

Five of the most widely used tissue:plasma partition coefficient methods were included in this investigation (Poulin and Theil, 2002; Berezhkovskiy, 2004; Rodgers *et al.*, 2005; Willmann

et al., 2005; Rodgers and Rowland, 2006; Schmitt, 2008). All of these methods require tissue composition data and physicochemical drug properties as inputs, but vary in type and quantity of data. Some of the methods have multiple equations to account for different classes of drugs or types of tissues.

Poulin and Theil method

The PT method uses drug solubility and the binding of the drug to macromolecules to predict tissue:plasma partition coefficients (Poulin and Theil, 2002). Eq. 1a gives the partition coefficient for non-adipose tissue,

$$K_p = \frac{P_{o:w}(f_{nlt} + 0.3f_{pht}) + (f_{wt} + 0.7f_{pht})}{P_{o:w}(f_{nlp} + 0.3f_{php}) + (f_{wp} + 0.7f_{php})} \frac{fu_p}{fu_t} \ , \quad (1a)$$

where $P_{o:w}$ is the *n*-octanol:buffer partition coefficient of the nonionized species at pH 7.4, f_{nl} is the fractional volume of neutral lipids, f_{ph} is the fractional volume of phospholipids, f_w is the fractional volume of water, and fu is the unbound fraction of drug. The subscripts t and p indicate tissue and plasma, respectively. Eq. 1b gives the adipose partition coefficient,

$$K_p = \frac{D^*_{o:w}(f_{nlt} + 0.3f_{pht}) + (f_{wt} + 0.7f_{pht})}{D^*_{o:w}(f_{nlp} + 0.3f_{php}) + (f_{wp} + 0.7f_{php})} \frac{fu_p}{1} \ , \quad (1b)$$

where $D^*_{o:w}$ is the olive oil:buffer partition coefficient of both the nonionized and ionized species at pH 7.4. Poulin and Theil had previously demonstrated that $D^*_{o:w}$ yields a better prediction for adipose tissue partition coefficients (Poulin *et al.*, 2001). Further, fu_t is set to one because macromolecular binding is negligible in adipose tissue. Poulin and Theil reported the steady state volume of distribution, V_{ss}, rather than K_p values. V_{ss} is given by

$$V_{ss} = \left(\sum V_t K_p\right) + V_e E:P + V_p \ ,$$

where V is the fractional body volume of a tissue (t), erythrocyte (e), and plasma (p), and $E:P$ is the erythrocyte:plasma ratio. $E:P$ is estimated as

$$E:P = \frac{BP - (1 - Ht)}{Ht} \ ,$$

where BP is the *in vitro* blood:plasma ratio and Ht is the hematocrit content in blood, assumed to be 45%.

Berezhkovskiy method

Berezhkovskiy derived a modified version of the PT method that does not require the assumption:

$$\frac{f_{wt} + 0.7f_{pht}}{f_{wp} + 0.7f_{php}} = 1 \ ,$$

but instead, only considered tissue binding in the water fraction according to the following equations (Berezhkovskiy, 2004):

$$K_p = \frac{P_{o:w}(f_{nlt} + 0.3f_{pht}) + \frac{f_{wt}}{fu_t} + 0.7f_{pht}}{P_{o:w}(f_{nlp} + 0.3f_{php}) + \frac{f_{wp}}{fu_p} + 0.7f_{php}} \ , \tag{2a}$$

$$K_p = \frac{D^*_{o:w}(f_{nlt} + 0.3f_{pht}) + \frac{f_{wt}}{fu_t} + 0.7f_{pht}}{D^*_{o:w}(f_{nlp} + 0.3f_{php}) + \frac{f_{wp}}{fu_p} + 0.7f_{php}} \ , \tag{2b}$$

where Eq. 2a and 2b give the partition coefficients for non-adipose tissue and adipose tissue, respectively.

Rodgers and Rowland method

Rodgers and Rowland developed two prediction methods: one for moderate-to-strong bases and zwitterions with $\mathrm{p}K_a \geq 7$, and one for acids, very weak bases, neutrals, and zwitterions with $\mathrm{p}K_a < 7$ (Rodgers *et al.*, 2005; Rodgers and Rowland, 2006). Rodgers and Rowland reported equations for steady-state tissue:plasma water partition coefficients (K_{pu}), so these were scaled by fu_p to calculate K_p. The equation for moderate-to-strong bases considered the partitioning of the drug into neutral lipids and phospholipids, the dissolution of

the drug into tissue water, and the electrostatic interactions with acidic tissue phospholipids. The partition coefficients are given by

$$K_p = \left(f_{ew} + \frac{1+X}{1+Y} f_{iw} + \frac{K a_{ap} f_{apl} X}{1+Y} + \frac{P f_{nl} + (0.3P + 0.7) f_{npl}}{1+Y} \right) f u_p \ , \quad (3a)$$

where f_{ew} is the fraction of extracellular water, f_{iw} is the fraction of intracellular water, f_{apl} is the fraction of acidic phospholipids, f_{nl} is the fraction of neutral lipids, f_{npl} is the fraction of neutral phospholipids, $K a_{ap}$ is the association constant between the drug and acidic phospholipids, and P is the *n*-octanol:buffer partition coefficient for non-adipose tissue and the olive oil:buffer partition coefficient for adipose tissue. X and Y are the ionization terms for the drug in intracellular water and plasma, respectively, and were calculated using the Henderson-Hasselbalch equation (Radić and Prkić, 2012). In the case of a monoprotic base, for example, $X = 10^{\mathrm{p}K_a - \mathrm{pH}_{iw}}$ and $Y = 10^{\mathrm{p}K_a - \mathrm{pH}_p}$, where pH_{iw} is the pH of intracellular water and pH_p is the pH of plasma.

The equation for acids, very weak bases, neutrals, and zwitterions with $\mathrm{p}K_a < 7$ incorporated partitioning into neutral lipids and phospholipids, the dissolution of the drug into tissue water, and associations with extracellular proteins. The partition coefficients are given by

$$K_p = \left(f_{ew} + \frac{1+X}{1+Y} f_{iw} + \frac{K a_{pr} f_{pr} X}{1+Y} + \frac{P f_{nl} + (0.3P + 0.7) f_{npl}}{1+Y} \right) f u_p \ , \quad (3b)$$

where f_{pr} is the fraction of albumin for acids, very weak bases, and zwitterions with $\mathrm{p}K_a < 7$ and the fraction of lipoprotein for neutral drugs.

Schmitt method

The Schmitt method explicitly considered the electrostatic interactions between charged molecules at physiological pH and acidic phospholipids (Schmitt, 2008). The lipid subcompartment consisted of neutral lipids, neutral phospholipids, and acidic phospholipids. The partition coefficients are given by

$$K_p = (f_w + K_{nl} f_{nl} + K_{npl} f_{npl} + K_{apl} f_{apl} + K_{pr} f_{pr}) f u_p \ , \quad (4)$$

where K_{npl} is the neutral phospholipids:water partition coefficient, K_{apl} is the acidic phospholipid:water partition coefficient, and K_{pr} is the protein:water partition coefficient.

PK-Sim Standard method

PK-Sim® software, which is part of the Open Systems Pharmacology Suite http://www.open-systems-pharmacology.org/, adopted a default partition coefficient calculation method proposed by Willmann and co-workers (Willmann *et al.*, 2005). This method incorporates partitioning into tissue water, lipids, and proteins where K_p is calculated as:

$$K_p = (f_w + K_{lipid} f_{lipid} + K_{pr} f_{pr}) f u_p \ . \quad (5)$$

All five methods were implemented as R script functions (R Core Team, n.d.) whose outputs were verified against partition coefficients reported in the corresponding papers (see associated Github repository https://github.com/metrumresearchgroup/PBPK_PC). Pearson correlation coefficients (PCCs) were calculated using predictions for strong bases, weak bases, acids, neutrals, and zwitterions. The papers reported predicted coefficients for different drugs, so the particular drugs used in the PCC calculation varied. Berezhkovskiy, Schmitt, and Willmann and co-workers did not report predicted partition coefficients or V_{ss} values. In these cases, PK-Sim software outputs for each of the three methods were used for verification.

To investigate the impact of different tissue compositions on predictions, K_p predictions from PT, Berez, Schmitt, and PK-Sim, using two drugs from each class (metoprolol, acebutolol-R, voriconazole, alprazolam, thiopental, phenobarbital, digoxin, ethoxybenzamide, ofloxacin, and enoxacin) and the originally reported respective tissue compositions, were compared against the same predictions from the RR reported tissue composition and PCCs were calculated. The RR reported tissue composition was the only one that could be swapped with

inputs of other methods because it alone included all of the necessary parameters for the remaining four methods.

Development of a standardized tissue composition database

Each tissue:plasma partition coefficient method included in this study used a different set of tissue composition information. While some of the methods used tissue composition for humans, other methods, such as RR, used tissue composition information from rats. Differences in predictions from the methods could have been due to both the tissue composition and the methods themselves, thereby confounding comparisons of the predictions from the five partition coefficient methods.

Since tissue composition influences tissue:plasma partition coefficient predictions, this study proposed a standardized tissue composition that can be used with each of the partition coefficient methods. The standardized tissue composition combined information from several sources to avoid biasing the evaluation of the partition coefficient methods (Open Systems Pharmacology, n.d.; Poulin and Theil, 2002; Rodgers *et al.*, 2005; Rodgers and Rowland, 2006; Ruark *et al.*, 2014). Human values for certain types of tissue composition were not found in literature, so values for rats were used in the standardized tissue composition. In particular, the f_{ew}, f_{iw}, pH, albumin ratio (AR), and lipoprotein ratio (LR) for all tissues, and f_{npl} for bone and gut were from rats (Rodgers *et al.*, 2005; Rodgers and Rowland, 2006). It was assumed that $f_{water} = f_{ew} + f_{iw}$ for all tissues except plasma and red blood cells (RBCs) that do not have f_{ew} and for these f_{water} values were taken from Ruark and co-workers. The standardized tissue composition was used as input for each partition coefficient method. Partition coefficient predictions from each method using the standardized tissue composition were compared to predictions from the same method using the corresponding reported tissue compositions. The PCC was calculated for each method using partition coefficients for all tissues for the same drugs used in the comparison in the previous section.

In addition to the analysis comparing the PBPK predictions using the standardized tissue composition, a parallel analysis was carried out using the originally reported tissue compositions for each of the calculation methods. This was done to evaluate bias possibly associated with any one of the methods that could arise from using the standardized tissue composition database.

PBPK model framework

The PBPK model used ordinary differential equations to describe well-mixed tissues that were linked by the blood system. The model assumed perfusion-rate-limited kinetics. A PBPK model including 15 tissue compartments was implemented for each drug in this study. The body for this model was composed of the following tissues: lung, adipose, bone, brain, heart, kidney, muscle, skin, liver, pancreas, spleen, and gut (Figure 2). The model also included compartments for venous blood and arterial blood, and a “rest of body” compartment that represented the remainder of the tissues not explicitly included in the model. The volume of the “rest of body” compartment was derived by subtracting the volumes of all other compartments from body weight, while the blood flow to this compartment was derived by subtracting the blood flows of all compartments entering into venous blood from the cardiac output. The model equations are discussed further in the Supplementary Information section. Model parameters, including tissue volumes and blood flows, body weight, cardiac output, and drug-specific parameters, are also in the Supplemental Information section (Tables S1 and S2).

The general PBPK model was implemented in R, using the open source package *mrgsolve* (R Core Team, n.d.; Elmokadem *et al.*, 2019; Gastonguay *et al.*, 2019). Tissue:plasma partition coefficients were predicted for the tested drugs using each method, and each set of partition coefficients was used as input in the PBPK model, resulting in five PBPK model predictions for each tested drug. The “rest of body” partition coefficient was calculated as the average of the non-adipose tissue:plasma partition coefficients. The PBPK model was used to

predict plasma concentration profiles for 11 drugs, and the predictions were compared with experimental data. The general PBPK model framework was modified for each drug to account for differences in administration route and clearance. Additional details about the model are described in the Supplementary Information section.

Drugs included in the study

Drugs were divided into five classes: strong bases, weak bases, acids, neutrals, and zwitterions. The division was made based on how the tissue:plasma partition coefficient methods account for differences in drugs. For example, RR accounts for different types of interactions between tissue components and strong and weak bases, but assumes that strong and weak acids have the same types of interactions with tissue components (Rodgers *et al.*, 2005; Rodgers and Rowland, 2006). Drugs were selected based on availability of published observed plasma concentrations and physicochemical parameters, including log*P*, $\mathrm{p}K_a$, BP, fu_p, clearance rates, and absorption rates. The strong bases investigated were metoprolol and caffeine, and the weak bases were voriconazole, alfentanil, nevirapine, and midazolam (Björkman *et al.*, 1998; Gaohua *et al.*, 2012; Zane and Thakker, 2014; De Sousa Mendes *et al.*, 2017; Elmokadem *et al.*, 2019). The acids were thiopental and nifedipine (Nguyen *et al.*, 1996; Ke *et al.*, 2012). The neutrals were digoxin and artemether, and the zwitterion was ofloxacin (Sumner and Russell, 1976; Flor *et al.*, 1993; Lin *et al.*, 2016). The Schmitt and PK-Sim Standard methods recommended the use of log*MA* (membrane affinity) in place of log*P* (Willmann *et al.*, 2005; Schmitt, 2008). Due to the limited availability of log*MA* values and to unify the input information for all methods, log*P* was used for all methods and all drugs in this investigation. The simulation scenarios for the tested drugs followed the published clinical protocols and were summarized in Table S3.

Evaluation of PBPK model predictions

Model predicted plasma concentration curves using the different calculation methods were compared with observed plasma concentrations procured from literature using WebPlotDigitizer (https://automeris.io/WebPlotDigitizer/). The percent root-mean-square error (RMSE) between the predicted drug plasma concentrations and the observed concentrations was defined as $RMSE = 100\frac{\sqrt{\frac{\sum_{i=1}^{n}(\hat{y}_i - y_i)^2}{n}}}{y_{max} - y_{min}}$, where $\hat{y}$ and y are the predicted and observed plasma concentrations, respectively, with each containing n values.

The R package *PKNCA (Denney et al., 2015)* was used to estimate the half-life values for the observed concentrations and each of the predicted concentration curves (Denney *et al.*, 2018). The half-life percent error was defined as $t_{\frac{1}{2}error} = 100\frac{\left|t_{\frac{1}{2}observed} - t_{\frac{1}{2}predicted}\right|}{t_{\frac{1}{2}observed}}$, respectively. For consistency, the RMSE and half-life errors were reported as percentages. The mean percent RMSE and half-life percent error were calculated for each method by taking the average of the values for each drug.

Results

Verification of R scripted implementations of the tissue:plasma partition coefficient prediction methods

The R scripted implementations of each of the tissue:plasma partition coefficient prediction methods were first verified against the reported partition coefficients in the respective publications (Figure 3). The input tissue compositions were extracted from the respective publications as well and so were different for each calculation method. The reported values that were used for verification were the PK-Sim generated human K_p values for Berez, Schmitt and PK-Sim, human V_{ss} values for PT, and rat K_{pu} values for RR (Figure 3). A correlation coefficient

of one was found for each method, indicating the scripts accurately reproduced the reported predictions (Figure 3).

Impact of different tissue compositions on K_p prediction methods outcome

Tissue composition information was a key input for each method, yet each method used different compositions. To demonstrate the impact of different tissue compositions on predictions, K_p predictions from PT, Berez, Schmitt and PK-Sim and the respective reported tissue compositions, were compared against the same predictions from the RR reported tissue composition (Figure 4). Swapping tissue compositions had a marked impact on the predicted K_p values from PT, Berez and Schmitt with PCC=0.28, 0.26, 0.62, respectively (Figure 4A-3C). The PK-Sim method appeared to be more robust while predicting K_p values from the varied tissue composition (PCC=0.94, Figure 4d).

Verification of the standardized tissue composition database

Table 1 contains the standardized tissue composition database. To verify that using the standardized tissue composition yielded biologically reasonable partition coefficients, predictions from each method using the reported tissue composition was plotted against predictions from the same method for the same drugs using the standardized tissue composition (Figure 5). PT (Figure 5A) and Berez (Figure 5B) produced similar predictions using the two different tissue compositions, where the PCC was 0.8 and 0.83, respectively. RR had the lowest correlation (PCC=0.32, Figure 5C). The Schmitt method produced very similar predictions using the two tissue compositions (PCC=0.96, Figure 5D) and the PK-Sim method produced seemingly identical predictions (PCC=1, Figure 5E).

Quantifying the impact of each tissue:plasma partition coefficient method on PBPK model outputs

Predictions of partition coefficients for each tissue were compared using a representative drug from each class: metoprolol (strong base), voriconazole (weak base), nifedipine (acid), digoxin (neutral), and ofloxacin (zwitterion) (Figure 6). The PT and Berez methods predicted smaller partition coefficients for every tissue in comparison to the other methods, and adipose had the greatest difference from the median (Figure 6A). The Schmitt and PK-Sim methods predicted the adipose partition coefficient for voriconazole to be an order of magnitude greater than the values predicted by the other methods (Figure 6B). For nifedipine, the PT method predicted the largest partition coefficients for all tissues except adipose, whereas the RR method predicted the smallest values for all tissues (Figure 6C). The Schmitt and PK-Sim methods had higher predictions for the adipose partition coefficient for digoxin (neutral) than the other methods (Figure 6D). The RR method predicted the highest partition coefficients for ofloxacin (zwitterion) for all tissues (Figure 6E). Predictions of partition coefficients were also compared for caffeine, alfentanil, midazolam, nevirapine, thiopental, and artemether (Figure S1). The RR method predicted the largest partition coefficients for all tissues for caffeine (Figure S1A). For alfentanil, the PT methods predicted the largest partition coefficients for most of the tissues (Figure S1B). The PK-Sim and Schmitt methods had the highest predictions for the adipose partition coefficient for midazolam, nevirapine, thiopental, and artemether (Figures S1B-F). Interestingly, the tissue:plasma partition coefficient for adipose was generally the most variable for every drug tested.

The PBPK model predictions for each partition coefficient method were compared with observed data for each drug (Figures 7 and S2). Notably, no model fitting was conducted for these predictions. The PBPK model predictions using the PT and Berez methods matched the metoprolol observations more closely early in the simulated profile (e.g., prior to approximately

five hours post dose) compared to later observations (Figure 7A). For voriconazole, the PBPK models using each method predicted similar plasma concentration profiles (Figure 7B). The PT method yielded a plasma concentration profile most similar to the observed data for nifedipine, whereas the RR method resulted in overprediction of the plasma concentration for the entire simulation time (Figure 7C). The Schmitt and PK-Sim methods yielded more accurate PBPK model predictions for digoxin than the other methods (Figure 7D). The RR method resulted in the most accurate PBPK model prediction for ofloxacin (Figure 7E). The RR method yielded the lowest plasma concentration profile for the simulation time for caffeine (Figure S2A). The simulated plasma concentration profiles were similar for all methods for alfentanil, midazolam, and artemether (Figures S2B-C,G), The Schmitt and PK-Sim methods underpredicted the plasma concentration profile for nevirapine (Figure S2D). The PK-Sim method yielded the plasma concentration profiles most similar to the observed data for S-thiopental and R-thiopental (Figures S2E-F).

Precision and bias metrics were measured for PBPK predictions using the standardized and reported tissue compositions (Table 2 and Figure 8). The results showed that no one partition coefficient estimation method consistently outperformed the others. When using the standardized tissue composition, the RR method performed best for ofloxacin, whereas the PT method resulted in the smallest errors for nifedipine. For the other 9 drugs, the results were mixed across the metrics. For example, digoxin PK prediction resulted in the smallest percent RMSE with Schmitt and the smallest half-life percent error with RR.

Generally, the estimated errors when using the reported tissue compositions were comparable to the ones estimated when using the standardized tissue compositions (Table 2, Figures 8 and 9). The only few exceptions were mostly related to the Schmitt method that seemed more sensitive to the tissue composition used in making the PBPK predictions than the other methods (Figure 9).

Discussion

Tissue:plasma partition coefficients are a key component in PBPK modeling, but are impractical to measure experimentally. The introduction of *in silico*, mechanistic-based methods to predict the coefficients was a considerable advancement in PBPK modeling; these methods alleviated the need for *in vivo* animal experiments to derive the partition values (Jones and Rowland-Yeo, 2013). Furthermore, mechanistic-based methods are generally based on human tissue composition, which carries a potential advantage over values experimentally determined using animal tissue composition. Since each of these methods uses different assumptions and different input information, each one can also produce different partition coefficient predictions. It was unclear if one method was superior for a certain class of drugs, or if no method was consistently more accurate than the others. In the context of PBPK modeling, it was then unclear which method should be used to predict plasma concentration profiles.

This study sought to compare the PBPK model predictions generated by five commonly used partition coefficient methods with observed data. The results from swapping tissue compositions demonstrated the impact of tissue compositions on partition coefficient predictions and highlighted the importance of reaching a standardized tissue composition to eliminate this additional source of variability while quantifying the impact of these different calculation methods on PBPK model predictions. A standardized tissue composition database was established and used in all of the partition coefficient prediction methods in the study. The standardized tissue composition provided a means for a quantitative comparison of these methods based solely on their underlying assumptions. Due to limitations in available data, values for f_{eu}, f_{iu}, AR, and LR for all tissues and f_{npl} for bone and gut were from rats, but the flexible implementation of the standardized tissue composition database ensures a mechanism for simple updating when the human data becomes available.

Partition coefficient predictions from each method using the reported tissue composition were compared to predictions using the standardized tissue composition. For the PT and Berez methods, the heart partition coefficient differed the most remarkably between the predictions using the reported and standardized tissue compositions. This difference likely resulted from differences between the fraction of neutral lipids in the heart in the reported and standardized tissue compositions. The RR method predictions had the lowest correlation, which was anticipated given that the reported tissue composition was measured in rats, whereas those in the standardized tissue composition were human. Further, the reported tissue compositions relevant to the Schmitt and PK-Sim methods were similar to the corresponding ones in the standardized tissue composition, so the close correlation between the predictions was expected. The results provided confidence in the K_p predictions generated using the standardized tissue composition and hence, the standardized tissue composition was used to calculate the partition coefficients for the remainder of this study.

Comparing the impact of the different partition coefficient calculation methods on PBPK model predictions was then carried out using the standardized tissue composition. As these calculation methods are often used prior to the availability of clinical data, the aim of the current work was not to further consider the subsequent estimation of these values from the available data. For example, the curated observed data (Figures 7 and S2) could be further considered through sensitivity analyses and subsequent parameter optimization of K_p following an approach similar to that recently described (Yau *et al.*, 2020). The outcomes of such an approach, however, would be highly reliant on the collection designs employed by each of the studies used for the example drugs. Such results, if conducted subsequent to the findings reported herein, may add to our understanding of extending PBPK models in the circumstances when clinical data are available.

This study considered the performance of the partition coefficient methods for different classes of drugs. For strong bases, weak bases, acids, and neutrals, no single partition coefficient method consistently produced PBPK model predictions that were more accurate than the other methods. In contrast, for zwitterions, the RR method appeared superior. However, due to the limited availability of data for zwitterionic drugs, only one drug was investigated, and, as such, further investigation is needed.

Notably, given that the individual partition coefficient calculation methods were optimized using the separate sets of reported tissue compositions, the PBPK predictions using the standardized tissue composition database might have been biased towards some of the methods with closer agreement between their reported tissue compositions and the standardized ones. A parallel analysis to investigate the impact of this possible bias was therefore undertaken. The resulting comparability of predictive performance (Table 2, Figures 8 and 9), regardless of method, between the standardized and original reported tissue compositions values further substantiated that a universal set of these values can be used without the need to switch them out specific to each partition coefficient calculation method. That is, a universal control set of tissue composition values can be used to assess the sensitivity to the partition coefficient calculation method. Generally, the error estimates from the PBPK predictions using the standardized versus the reported tissue compositions were close with no consistently better performance for using one of them (Table 2 and Figures 8 and 9).

Additional approaches have been developed to predict tissue:plasma partition coefficients. Endo and co-workers suggested a general method that used tissue composition information (fraction of storage lipids, membrane lipids, albumin, other proteins, and water), similar to the methods considered here (Endo *et al.*, 2013). The partition coefficients between phases (e.g. between storage lipids and water) were predicted using polyparameter linear free energy relationships, a type of multiple linear regression model. Unlike the other mechanistic-based methods, Freitas and co-workers suggested a machine learning approach to predicting

tissue:plasma partition coefficients (Endo *et al.*, 2013; Freitas *et al.*, 2015). Decision tree-based regression methods were implemented to predict partition coefficients, and, subsequently, the volume of distribution at steady state. Both methods seem to provide accurate predictions of tissue:plasma partition coefficients. This study investigated the most commonly used methods, but these and other methods could be included in future analyses.

The results of this study demonstrated that no method was consistently superior to the others, even within classes of drugs. This highlights the need to include the process of choosing the suitable method as part of the optimization process during PBPK model development. Using the presented R implementation of the five most popular calculation methods as well as the standardized tissue composition database would make the comparison, sensitivity, and optimization steps much more accessible, and, thus, could eventually be part of the PBPK model-building routine.

Acknowledgements

None

Authorship Contributions

Participated in research design: Utsey, Riggs, and Elmokadem

Conducted experiments: Utsey, Gastonguay, Russel, Freling, and Elmokadem

Contributed new reagents or analytic tools: NA

Performed data analysis: Utsey

Wrote or contributed to the writing of the manuscript: Utsey, Riggs, and Elmokadem

References

Arundel PA (1997) A Multi-Compartmental Model Generally Applicable to Physiologically-Based Pharmacokinetics. *IFAC Proceedings Volumes* **30**:129–133.

Berezhkovskiy LM (2004) Volume of distribution at steady state for a linear pharmacokinetic system with peripheral elimination. *J Pharm Sci* **93**:1628–1640.

Björkman S, Wada DR, and Stanski DR (1998) Application of physiologic models to predict the influence of changes in body composition and blood flows on the pharmacokinetics of fentanyl and alfentanil in patients. *Anesthesiology* **88**:657–667.

Denney B, Buckeridge C, and Duvvuri S (2018) Perform Pharmacokinetic Non-Compartmental Analysis.

Denney WS, Duvvuri S, and Buckeridge C (2015) Simple, Automatic Noncompartmental Analysis: The PKNCA R Package.

De Sousa Mendes M, Lui G, Zheng Y, Pressiat C, Hirt D, Valade E, Bouazza N, Foissac F, Blanche S, Treluyer J-M, Urien S, and Benaboud S (2017) A Physiologically-Based Pharmacokinetic Model to Predict Human Fetal Exposure for a Drug Metabolized by Several CYP450 Pathways. *Clin Pharmacokinet* **56**:537–550.

Elmokadem A, Riggs MM, and Baron KT (2019) QSP and PBPK Modeling with mrgsolve: A Hands-on Tutorial. *CPT Pharmacometrics Syst Pharmacol*, doi: 10.1002/psp4.12467.

Endo S, Brown TN, and Goss K-U (2013) General model for estimating partition coefficients to organisms and their tissues using the biological compositions and polyparameter linear free energy relationships. *Environ Sci Technol* **47**:6630–6639.

Flor SC, Rogge MC, and Chow AT (1993) Bioequivalence of oral and intravenous ofloxacin after multiple-dose administration to healthy male volunteers. *Antimicrob Agents Chemother* **37**:1468–1472.

Freitas AA, Limbu K, and Ghafourian T (2015) Predicting volume of distribution with decision tree-based regression methods using predicted tissue:plasma partition coefficients. *J Cheminform* **7**:6.

Gaohua L, Abduljalil K, Jamei M, Johnson TN, and Rostami-Hodjegan A (2012) A pregnancy physiologically based pharmacokinetic (p-PBPK) model for disposition of drugs metabolized by CYP1A2, CYP2D6 and CYP3A4. *Br J Clin Pharmacol* **74**:873–885.

Gastonguay MS, Russell S, Freling R, Riggs M, Kay K, Utsey K, and Elmokadem A (2019) Development of an open-source physiologically-based pharmacokinetic model to predict maternal-fetal exposures of CYP450-metabolized drugs.

Graham H, Walker M, Jones O, Yates J, Galetin A, and Aarons L (2012) Comparison of in-vivo and in-silico methods used for prediction of tissue: plasma partition coefficients in rat. *J Pharm Pharmacol* **64**:383–396.

Jansson R, Bredberg U, and Ashton M (2008) Prediction of Drug Tissue to Plasma Concentration Ratios Using a Measured Volume of Distribution in Combination With

Lipophilicity. *J Pharm Sci* **97**:2324–2339.

Jones H, and Rowland-Yeo K (2013) Basic concepts in physiologically based pharmacokinetic modeling in drug discovery and development. *CPT Pharmacometrics Syst Pharmacol* **2**:e63.

Ke AB, Nallani SC, Zhao P, Rostami-Hodjegan A, and Unadkat JD (2012) A PBPK Model to Predict Disposition of CYP3A-Metabolized Drugs in Pregnant Women: Verification and Discerning the Site of CYP3A Induction. *CPT Pharmacometrics Syst Pharmacol* **1**:e3.

Lin W, Heimbach T, Jain JP, Awasthi R, Hamed K, Sunkara G, and He H (2016) A Physiologically Based Pharmacokinetic Model to Describe Artemether Pharmacokinetics in Adult and Pediatric Patients. *J Pharm Sci* **105**:3205–3213.

Nguyen KT, Stephens DP, McLeish MJ, Crankshaw DP, and Morgan DJ (1996) Pharmacokinetics of thiopental and pentobarbital enantiomers after intravenous administration of racemic thiopental. *Anesth Analg* **83**:552–558.

Open Systems Pharmacology (n.d.).

Poulin P, Schoenlein K, and Theil FP (2001) Prediction of adipose tissue: plasma partition coefficients for structurally unrelated drugs. *J Pharm Sci* **90**:436–447.

Poulin P, and Theil F (2002) Prediction of Pharmacokinetics Prior to In Vivo Studies. 1. Mechanism-Based Prediction of Volume of Distribution. *J Pharm Sci* **91**:129–156.

Poulin P, and Theil F-P (2009) Development of a novel method for predicting human volume of distribution at steady-state of basic drugs and comparative assessment with existing methods. *J Pharm Sci* **98**:4941–4961.

Radić N, and Prkić A (2012) Historical remarks on the Henderson-Hasselbalch equation: its advantages and limitations and a novel approach for exact pH calculation in buffer region.

R Core Team (n.d.) R: A Language and Environment for Statistical Computing, Vienna, Austria.

Rodgers T, Leahy D, and Rowland M (2005) Physiologically based pharmacokinetic modeling 1: predicting the tissue distribution of moderate-to-strong bases. *J Pharm Sci* **94**:1259–1276.

Rodgers T, and Rowland M (2006) Physiologically based pharmacokinetic modelling 2: predicting the tissue distribution of acids, very weak bases, neutrals and zwitterions. *J Pharm Sci* **95**:1238–1257.

Ruark CD, Hack CE, Robinson PJ, Mahle DA, and Gearhart JM (2014) Predicting passive and active tissue:plasma partition coefficients: interindividual and interspecies variability. *J Pharm Sci* **103**:2189–2198.

Schmitt W (2008) General approach for the calculation of tissue to plasma partition coefficients. *Toxicol In Vitro* **22**:457–467.

Sumner DJ, and Russell AJ (1976) Digoxin pharmacokinetics: multicompartmental analysis and its clinical implications. *Br J Clin Pharmacol* **3**:221–229.

Valentin J (2002) Basic anatomical and physiological data for use in radiological protection:

reference values. *Ann ICRP* **32**:1–277.

Willmann S, Lippert J, and Schmitt W (2005) From physicochemistry to absorption and distribution: predictive mechanistic modelling and computational tools. *Expert Opin Drug Metab Toxicol* **1**:159–168.

Yau E, Olivares-Morales A, Gertz M, Parrott N, Darwich AS, Aarons L, and Ogungbenro K (2020) Global Sensitivity Analysis of the Rodgers and Rowland Model for Prediction of Tissue: Plasma Partitioning Coefficients: Assessment of the Key Physiological and Physicochemical Factors That Determine Small-Molecule Tissue Distribution. *AAPS J* **22**:41.

Zane NR, and Thakker DR (2014) A physiologically based pharmacokinetic model for voriconazole disposition predicts intestinal first-pass metabolism in children. *Clin Pharmacokinet* **53**:1171–1182.

Zhuang X, and Lu C (2016) PBPK modeling and simulation in drug research and development. *Acta Pharm Sin B* **6**:430–440.

Footnotes

Financial support

This work received no external funding.

Citation of meeting abstract

Utsey K, Gastonguay MS, Russell S, Freling R, Riggs MM, and Elmokadem A. Impact of Partition Coefficient Prediction Methods on PBPK Model Output Using a Unified Tissue Composition, ACoP10, Orlando FL, ISSN:2688-3953, 2019, Vol 1

Figure legends

Figure 1. The analysis workflow.

Figure 2. Schematic for the general, flow-limited, physiologically-based pharmacokinetic model. The drug can be cleared from the kidney and liver compartments. Tissues that are not explicitly included in the model are represented by the “Rest of body” compartment.

Figure 3. Verification of the open-source R script predictions with reported prediction values for each method. The PCC for each method is denoted by *r*. (A) Comparison between V_{ss} values calculated from the PT K_p values and the reported V_{ss} predictions. (B) Comparison between K_p values calculated by the Berez script and K_p values predicted using the Berez method within PK-Sim. (C) Comparison between K_{pu} predictions from the RR script and the reported K_{pu} values. (D) Comparison between K_p values from the Schmitt script and K_p values predicted using the Schmitt method within PK-Sim. (E) Comparison between K_p values from the PK-Sim script and K_p values predicted using the PK-Sim method within PK-Sim. The scripts reproduce partition coefficient predictions for all five methods.

Figure 4. Comparison between the tissue:plasma partition coefficients predicted using the corresponding reported tissue compositions for the select methods and the tissue composition reported by RR. The PCC for each method is denoted by *r*. (A-D) Comparisons of predictions from the PT, Berez, Schmitt, and PK-Sim methods, respectively. Predictions from each method are impacted by the use of different tissue compositions.

Figure 5. Comparison between predicted tissue:plasma partition coefficients (K_p) using the standardized tissue composition and the reported tissue compositions. The PCC for each

method is denoted by *r*. (A-E) Comparisons of predictions from the PT method, Berez method, RR method, Schmitt method, and PK-Sim methods, respectively.

Figure 6. Comparison of tissue:plasma partition coefficients (K_p) predicted by each method; a representative drug from each class is considered. The horizontal bars indicate the median partition coefficient for each tissue. (A-E) Partition coefficients are compared for metoprolol (strong base), voriconazole (weak base), nifedipine (acid), digoxin (neutral), and ofloxacin (zwitterion). The PT and Berez methods predict nearly identical partition coefficients.

Figure 7. Comparison between PBPK model prediction curves for each method and observed data for (A) metoprolol (10 mg IV) (Gaohua *et al.*, 2012) (B) voriconazole (4 mg/kg IV infusion) (Zane and Thakker, 2014) (C) nifedipine (10 mg PO) (Ke *et al.*, 2012) (D) digoxin (0.013 mg IV) (Sumner and Russell, 1976) (E) ofloxacin (400 mg IV) (Flor *et al.*, 1993). Dots indicate mean, and error bars indicate standard deviation of the observed plasma concentrations.

Figure 8. Comparison of the RMSE and half-life percent errors for each partition coefficient method and each drug. (A) and (B) are the RMSE percent errors calculated when using the standardized and reported tissue composition (TC), respectively. (C) and (D) are the half-life percent errors calculated when using the standardized and reported TC, respectively.

Figure 9. Comparison of the percent RMSE (top) and half-life error percent (bottom) calculated when using the standardized and reported TC on linear (A and C) and log (B and D) scales.

Tables

Table 1. Standardized tissue composition values are from Ruark and co-workers, unless indicated otherwise (Ruark *et al.*, 2014).

Tissue	f_{water}	f_{lipid}	f_{pr}	f_{pl} (Poulin *et al.*, 2001)	f_{nl}	f_{npl}	f_{apl}	pH (Schmitt, 2008)	f_{ew} (Rodgers *et al.*, 2005)	f_{iw} (Rodgers *et al.*, 2005)	AR (Rodgers *et al.*, 2005)	LR (Rodgers *et al.*, 2005)
Bone	0.446(Rodgers *et al.*, 2005)	0.268 (Open Systems Pharmacology, n.d.)	0.268 (Open Systems Pharmacology, n.d.)	0.0011	0.074 (Poulin *et al.*, 2001)	0.0016 (Rodgers and Rowland, 2006)	8E-04 (Open Systems Pharmacology, n.d.)	7	0.1	0.346	0.1	0.05
Brain	0.782(Rodgers *et al.*, 2005)	0.107	0.08	0.0565	0.045	0.0553	0.02022	7.1	0.162	0.620	0.048	0.041
Adipose	0.152(Rodgers *et al.*, 2005)	0.800	0.05	0.002	0.798	0.0478	0.0067	7.1	0.135	0.017	0.049	0.069
Heart	0.776(Rodgers *et al.*, 2005)	0.1	0.17	0.0166	0.089	0.0079	0.00309	7.1	0.32	0.456	0.157	0.16
Kidney	0.756(Rodgers *et al.*, 2005)	0.052	0.17	0.0162	0.036	0.0166	0.00387	7.22	0.273	0.483	0.13	0.137
Gut	0.757(Rodgers *et al.*, 2005)	0.062 (Open Systems Pharmacology, n.d.)	0.133 (Open Systems Pharmacology, n.d.)	0.0163	0.0487 (Poulin *et al.*, 2001)	0.0124 (Rodgers and Rowland, 2006)	3.5E-03 (Open Systems Pharmacology, n.d.)	7.4	0.282	0.475	0.158	0.141
Liver	0.734(Rodgers *et al.*, 2005)	0.067	0.18	0.0252	0.037	0.0115	0.00258	7.23	0.161	0.573	0.086	0.161
Lung	0.782(Rodgers *et al.*, 2005)	0.01	0.18	0.009	0.003	0.0056	0.0014	6.6	0.336	0.446	0.212	0.168
Muscle	0.748(Rodgers *et al.*, 2005)	0.019	0.17	0.0072	0.013	0.0092	0.0019	6.81	0.118	0.63	0.064	0.059
Skin	0.673(Rodgers *et al.*, 2005)	0.1	0.29	0.0111	0.036	0.0502	0.01382	7.0	0.382	0.291	0.277	0.096
Spleen	0.786(Rodgers *et al.*, 2005)	0.028	0.19	0.0198	0.014	0.0103	0.00191	7.0	0.207	0.579	0.097	0.207
Plasma	0.928	0.009	0.07	0.00225	0.003	0.0050	9.7E-04	7.3	-	-	0.029	6E-04
RBCs	0.663	0.005	0.33	-	0.002	0.0025	5E-05	7.2	-	0.663	-	-

f_{water} is the fractional volume of water, f_{lipid} is the fractional volume of lipid, f_{pr} is fractional volume of protein, f_{pl} is fractional volume of phospholipids, f_{nl} is fractional volume of neutral lipids, f_{npl} is fractional volume of neutral phospholipids, f_{apl} is fractional volume of acidic phospholipids, f_{ew} and f_{iw} represent extracellular and intracellular water, respectively, AR is albumin ratio, and LR is lipoprotein ratio.

DMD Fast Forward. Published on July 14, 2020 as DOI: 10.1124/dmd.120.090498

Table 2. Percent RMSE and half-life errors for each partition coefficient method and each drug.

	Percent RMSE										Half-life percent error									
	Standardized TC					Reported TC					Standardized TC					Reported TC				
	PT	Berez	RR	Schmitt	PK-Sim	PT	Berez	RR	Schmitt	PK-Sim	PT	Berez	RR	Schmitt	PK-Sim	PT	Berez	RR	Schmitt	PK-Sim
Metoprolol	151	152	142	142	145	157	157	141	142	145	40.5	41.5	76.4	67.3	141	42.5	43.4	30.2	169	175
Caffeine	21.4	21.5	30.4	26.7	22.1	21.2	21.5	24.9	31.7	21.9	39.0	42.6	82.0	65.8	118	40.6	44.7	13.4	15.0	119
Voriconazole	18.1	17.8	20.7	24.3	24.2	19.9	19.7	17.5	34.0	23.3	225	218	273	408	456	228	223	153	2610	435
Alfentanil	45.3	49.5	53.1	49.0	50.1	47.0	50.5	54.9	40.4	49.8	143	35.7	10.9	419	331	154	43.0	4.62	1360	332
Nevirapine	26.5	25.1	25.2	40.2	42.3	29.3	26.7	31.9	62.7	41.6	45.4	63.4	77.3	661	544	67.4	84.6	128	111	524
Midazolam	50.6	50.6	50.6	50.6	50.6	50.6	50.6	50.5	50.6	50.6	24.8	47.1	57.7	12.1	15.8	42.8	43.6	71.3	3.31	19.2
S-Thiopental	5.02	4.82	5.35	5.11	5.49	4.72	4.74	7.57	8.90	5.44	293	246	158	98.9	229	292	253	115	255	282
R-Thiopental	4.25	5.54	7.87	4.13	3.39	5.43	6.30	11.4	4.54	3.44	261	220	139	106	255	259	226	103	284	315
Nifedipine	24.0	111	1280	445	90.9	20.2	99.9	1280	30.9	74.6	22.0	16.6	73.7	101	307	33.5	5.26	73.9	21.8	288
Digoxin	17.9	18.3	20.4	11.4	13.2	17.7	18.1	24.7	37.9	13.0	177	163	126	219	312	188	171	89.7	1150	313
Artemether	30.2	21.8	21.4	29.9	35.6	27.4	21.4	48.2	63.3	35.4	39.2	39.6	44.4	19.3	5.69	56.8	48.9	34.0	41.3	1.15
Ofloxacin	23.5	23.2	6.38	24.0	23.4	23.3	23.1	10.9	12.0	21.9	59.3	59.0	19.3	59.8	59.2	59.1	59.0	37.0	40.2	57.5
Mean	34.9	41.7	139	71.1	42.2	35.3	41.6	142	43.2	40.5	114	99.3	94.8	186	231	122	104	71.1	505	239

RMSE is the root-mean-square error between the predicted drug plasma concentrations and the observed concentrations, PT is the Poulin and Theil prediction method, Berez is the Berezhkovskiy prediction method, RR is the Rogers and Roland prediction method, Schmitt is the Schmitt prediction method, and PK-Sim is the default PK-Sim prediction method.

DMD Fast Forward. Published on July 14, 2020 as DOI: 10.1124/dmd.120.090498
This article has not been copyedited and formatted. The final version may differ from this version.

Figures

Figure 1

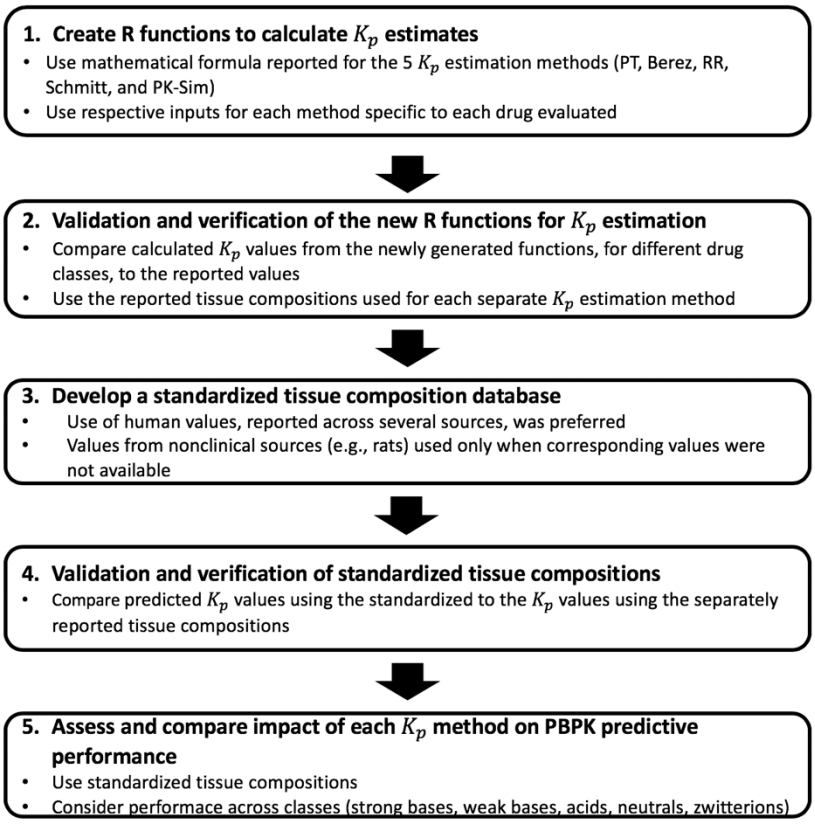

DMD Fast Forward. Published on July 14, 2020 as DOI: 10.1124/dmd.120.090498
This article has not been copyedited and formatted. The final version may differ from this version.

Figure 2

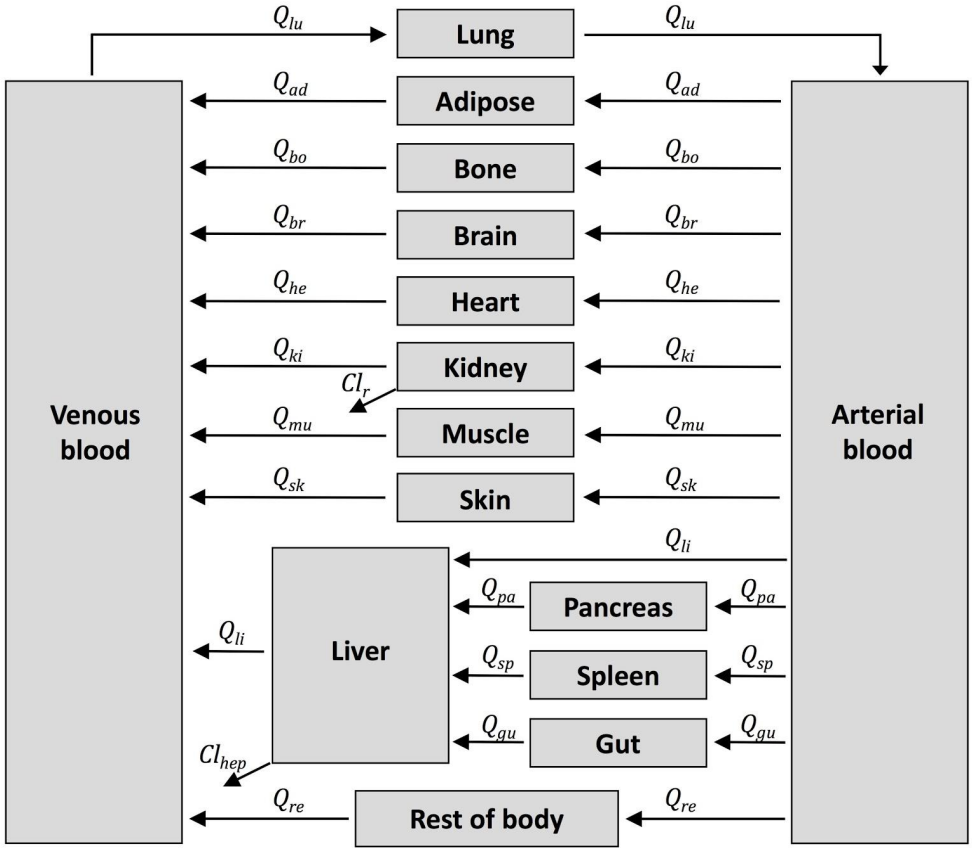

DMD Fast Forward. Published on July 14, 2020 as DOI: 10.1124/dmd.120.090498
This article has not been copyedited and formatted. The final version may differ from this version.

Figure 3

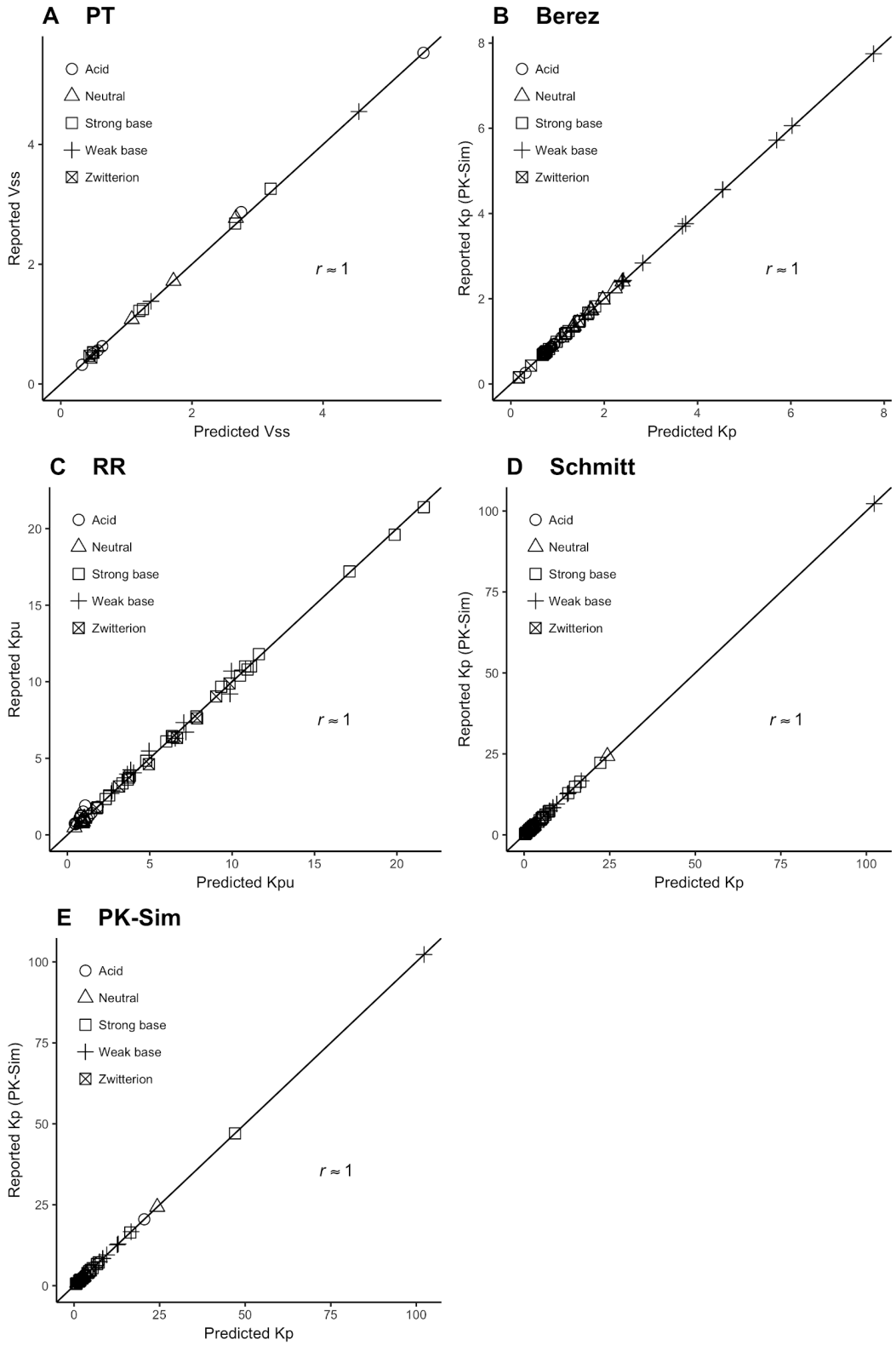

DMD Fast Forward. Published on July 14, 2020 as DOI: 10.1124/dmd.120.090498
This article has not been copyedited and formatted. The final version may differ from this version.

Figure 4

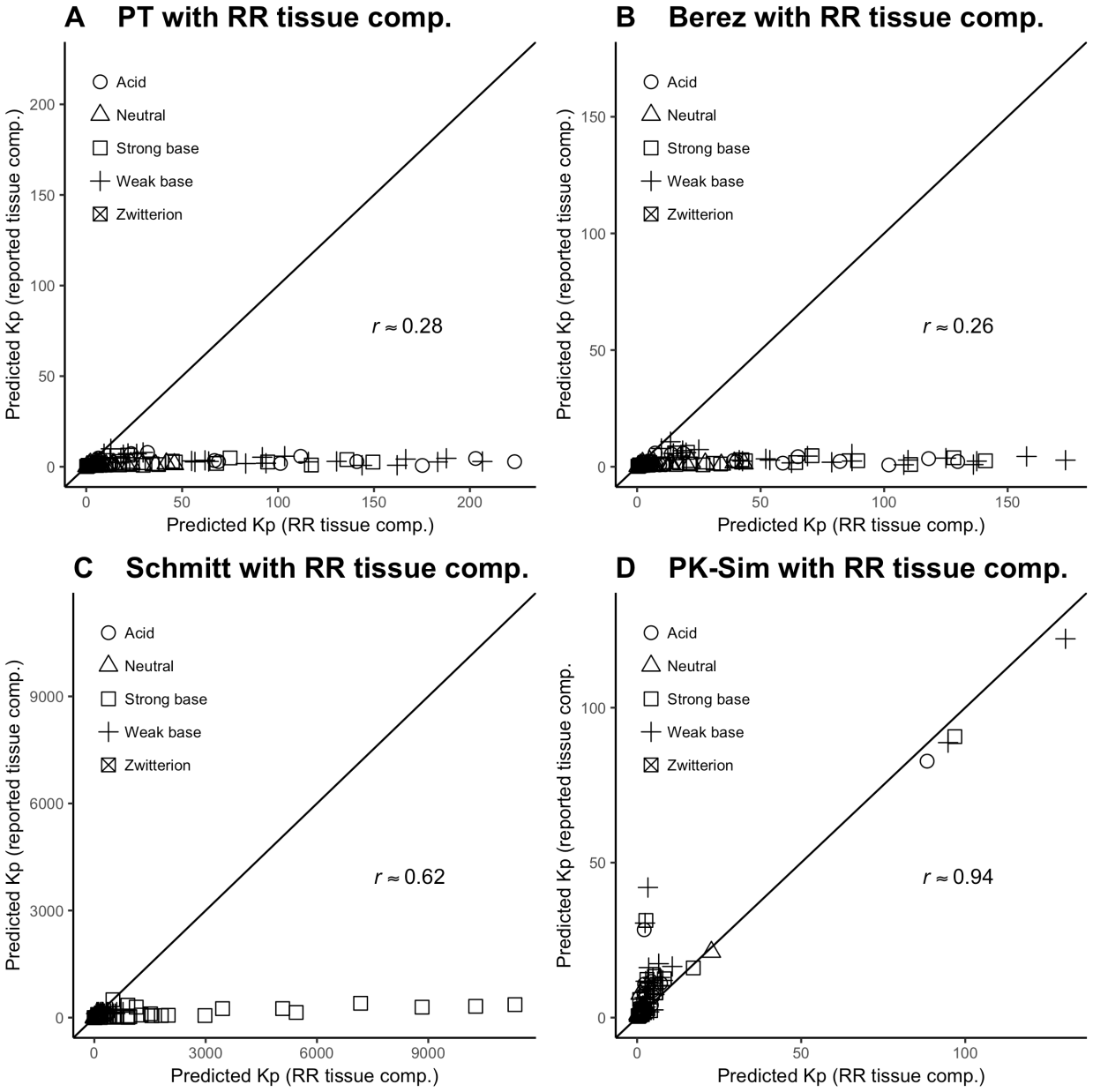

DMD Fast Forward. Published on July 14, 2020 as DOI: 10.1124/dmd.120.090498
This article has not been copyedited and formatted. The final version may differ from this version.

Figure 5

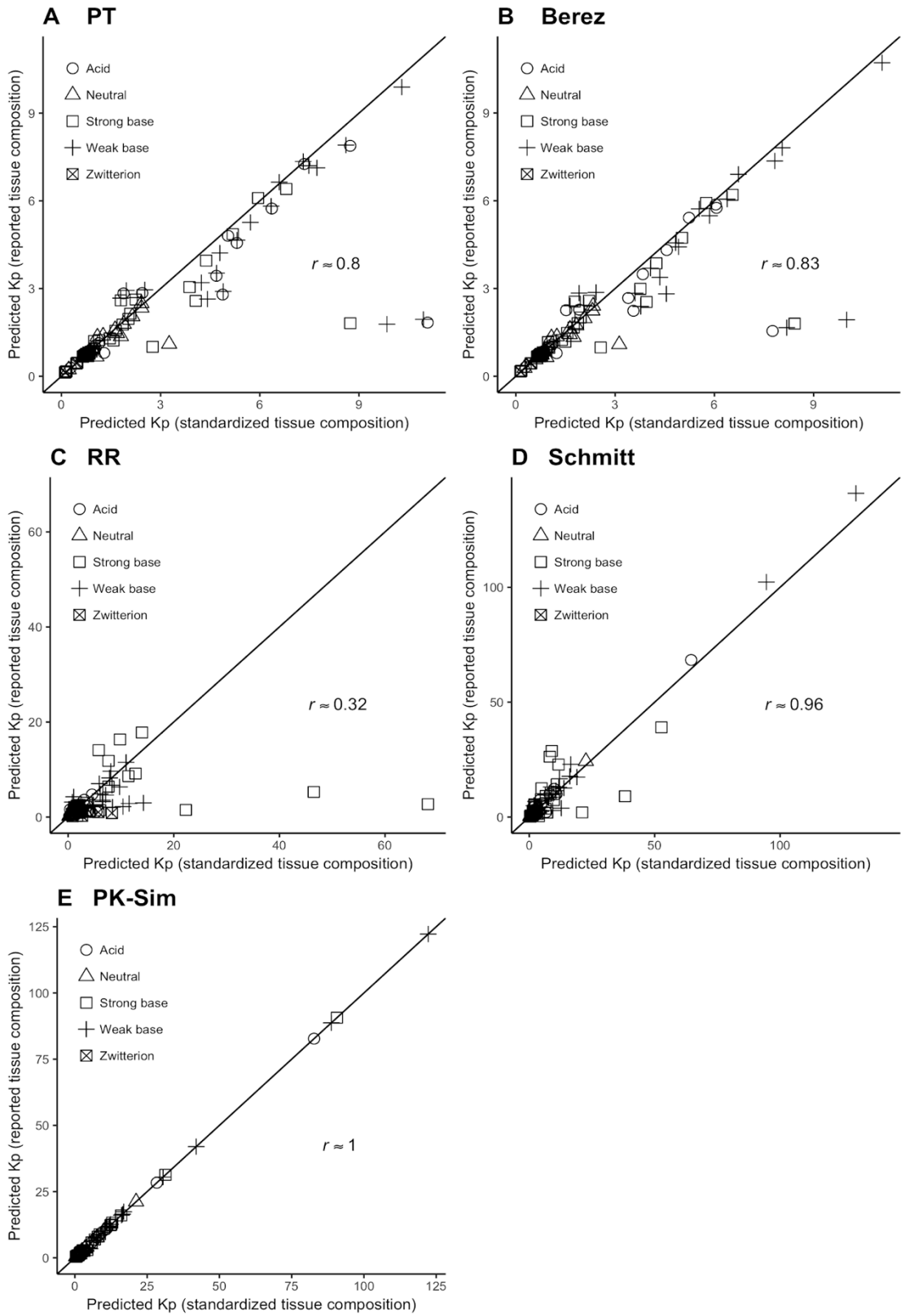

DMD Fast Forward. Published on July 14, 2020 as DOI: 10.1124/dmd.120.090498
This article has not been copyedited and formatted. The final version may differ from this version.

Figure 6

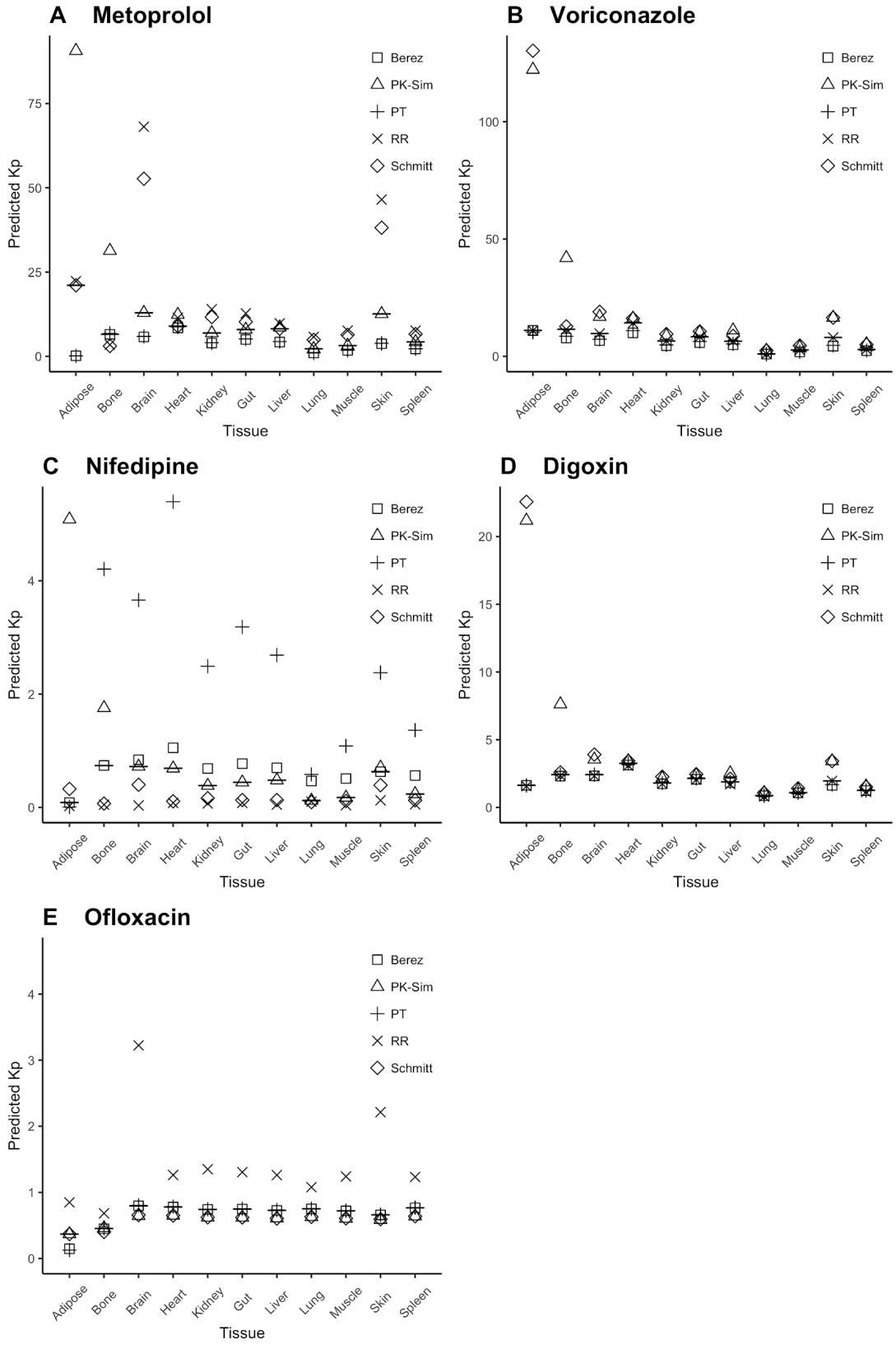

DMD Fast Forward. Published on July 14, 2020 as DOI: 10.1124/dmd.120.090498
This article has not been copyedited and formatted. The final version may differ from this version.

Figure 7

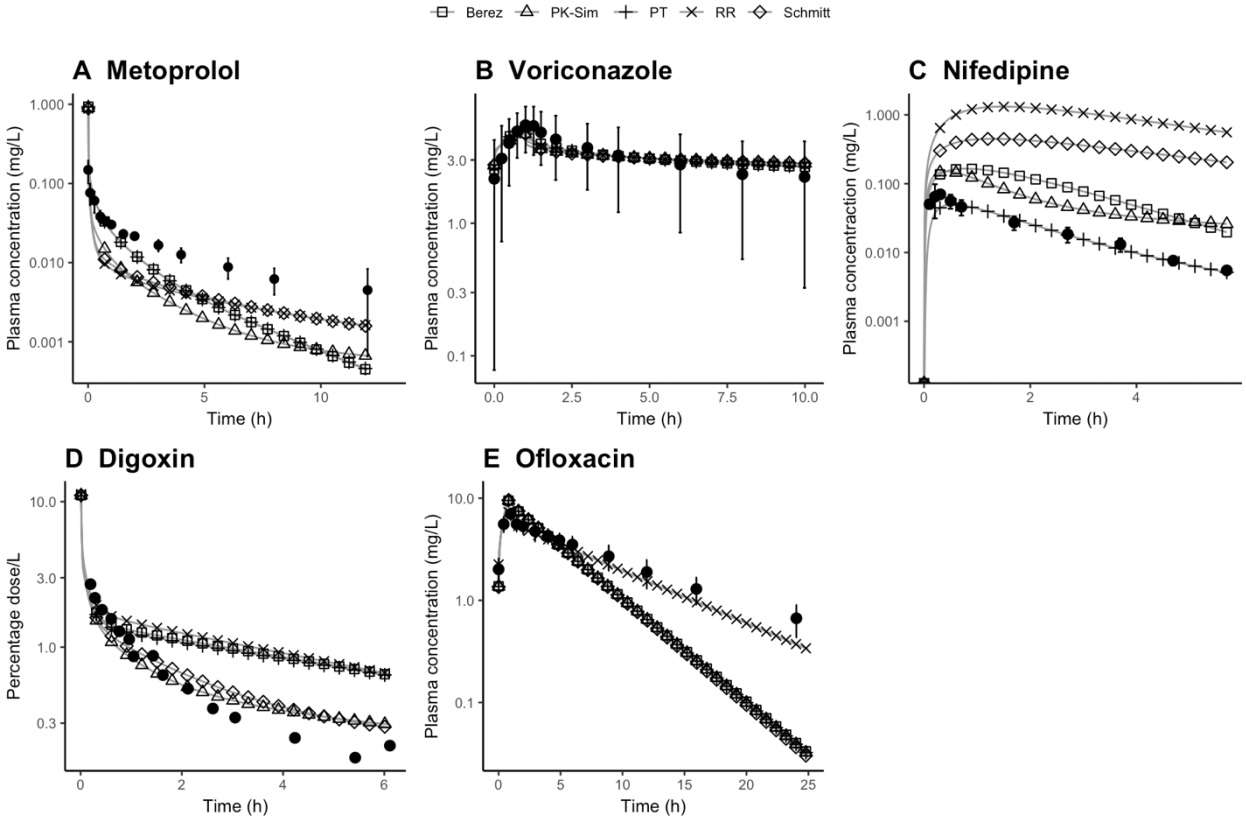

DMD Fast Forward. Published on July 14, 2020 as DOI: 10.1124/dmd.120.090498
This article has not been copyedited and formatted. The final version may differ from this version.

Figure 8

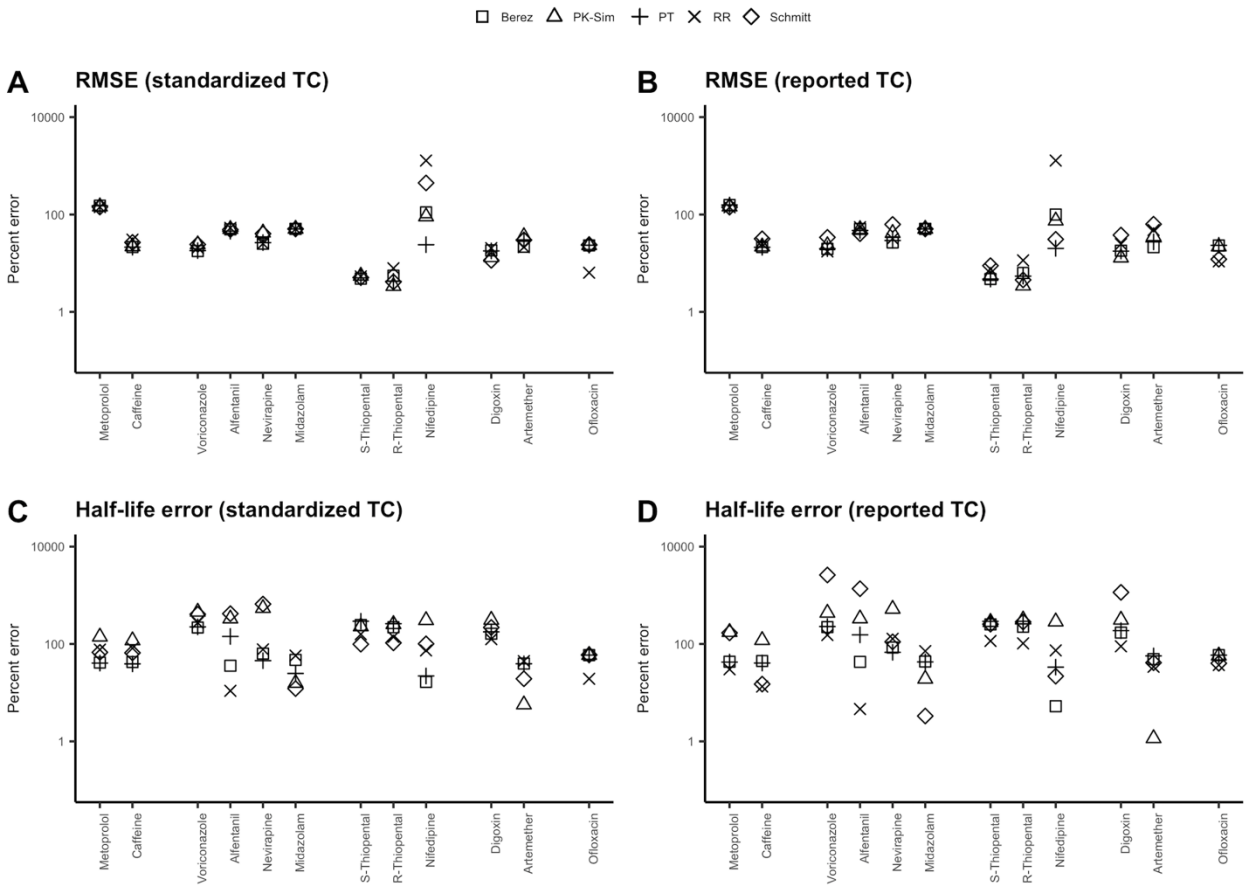

DMD Fast Forward. Published on July 14, 2020 as DOI: 10.1124/dmd.120.090498
This article has not been copyedited and formatted. The final version may differ from this version.

Figure 9

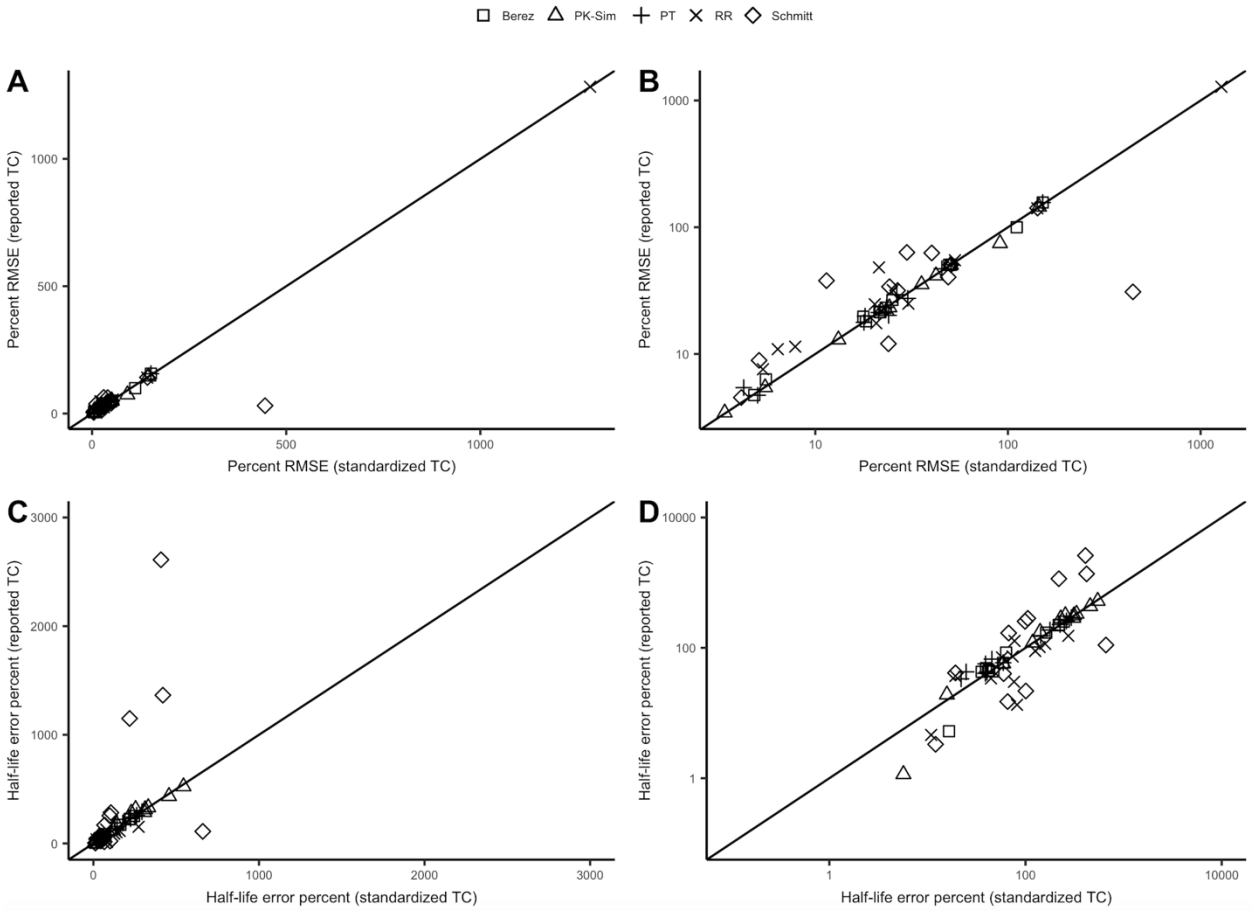

Supplemental Information

Quantification of the Impact of Partition Coefficient Prediction Methods on PBPK Model Output Using a Standardized Tissue Composition

Kiersten Utsey[1,2], Madeleine S Gastonguay[1,3], Sean Russell[1,4], Reed Freling[1,5], Matthew M Riggs[1], Ahmed Elmokadem[1]

[1]Metrum Research Group, Tariffville, CT, USA; [2]University of Utah, Salt Lake City, UT, USA; [3]University of Connecticut, Storrs, CT, USA; [4]University of Michigan, Ann Arbor, MI, USA; [5]Cornell University, Ithaca, NY, USA

Supplemental Methods

PBPK model equations

The flow-limited tissue compartments shown in Figure 2 are modeled using mass-balance ordinary differential equations. The general PBPK model framework used to model all of the drugs in this study is described by Eq. S1-S5 (Zhuang and Lu, 2016; Elmokadem *et al.*, 2019). The amount of drug in each non-eliminating tissue (adipose, bone, brain, heart, muscle, skin, pancreas, spleen, gut, and rest of body) is modeled using Eq. S1,

$$\frac{dA_T}{dt} = Q_T \left(C_A - \frac{C_T}{\frac{Kp_T}{BP}} \right) \quad . \tag{S1}$$

The subscript T refers to the tissue and A, Q, C and Kp represent drug amount, flow rate, drug concentration and tissue:plasma partition coefficient, respectively. C_A is the drug concentration in arterial blood compartment and BP is the blood:plasma concentration ratio.

The amount of drug in eliminating tissues (kidney and liver) is modeled using Eq. S2,

$$\frac{dA_T}{dt} = Q_T \left(C_A - \frac{C_T}{\frac{Kp_T}{BP}} \right) - Cl_T fu \frac{C_T}{\frac{Kp_T}{BP}} \ , \tag{S2}$$

where Cl_T is tissue clearance and fu is the fraction of unbound drug.

The amount of drug in arterial and venous blood are modeled using Eq. S3 and S4, respectively,

$$\frac{dA_A}{dt} = Q_{Lu}\left(\frac{C_{Lu}}{\frac{Kp_{Lu}}{BP}} - C_A\right) \tag{S3}$$

$$\frac{dA_V}{dt} = \sum_{T \neq Lu}\left(Q_T \frac{C_T}{\frac{Kp_T}{BP}}\right) - Q_{Lu}C_V \ , \tag{S4}$$

where A_A is the amount of drug in arterial blood and A_V is the amount of drug in venous blood.

The amount of drug in lungs, A_{Lu}, is modeled using Eq. S5,

$$\frac{dA_{Lu}}{dt} = Q_{Lu}\left(C_V - \frac{C_{Lu}}{\frac{Kp_{Lu}}{BP}}\right) \ . \tag{S5}$$

The general PBPK model described by Eq. S1-S5 was modified to account for differences between the drugs.

Drugs administered orally include a dose compartment, D, which accounts for the delay between oral administration and passage into the gut circulation. The models for nifedipine, midazolam, caffeine, and artemether include Eq. S6,

$$\frac{dD}{dt} = -K_a D \ , \tag{S6}$$

which governs the dynamics of the dose compartment.

The hepatic clearance for voriconazole is calculated as

$$Cl_{hep} = \frac{V_{max,Li}}{K_{m,Li}} \frac{MPPGL}{f_{umic}} W_{Li} \ , \tag{S7}$$

where $V_{max,Li}$ and $K_{m,Li}$ are the hepatic maximum rate and Michaelis-Menten constant estimated from the *in vitro* microsomal system, $MPPGL$ is the mg microsomal proteins per gram liver, f_{umic} is the free fraction of the drug in the *in vitro* microsomal system, and W_{Li} is the liver weight (Elmokadem *et al.*, 2019).

PBPK model parameters

The models use a body weight of 60 and 73 kg and total cardiac output of 5.9 and 6.5 L/min for females and males, respectively (Valentin, 2002). Tissue volume and blood flow parameters are compiled in Table S1. The nevirapine and artemether studies were conducted in males, so the male parameters were used in the corresponding PBPK models (Lin *et al.*, 2016; De Sousa Mendes *et al.*, 2017).

Table S1. Tissue volumes and blood flows for females and males (Valentin, 2002).

	Tissue volume (L)		Tissue blood flow (fraction of cardiac output)	
Tissue	Females	Males	Females	Males
Adipose	22.5	18.2	0.085	0.05
Bone	7.8	10.5	0.05	0.05
Brain	1.3	1.45	0.12	0.12
Gut	1.03	1.3	0.17	0.15
Heart	0.25	0.33	0.05	0.04
Kidney	0.275	0.31	0.17	0.19
Liver	1.4	1.8	0.27	0.255
Lung	0.42	0.5	1	1
Muscle	17.5	29	0.12	0.17
Skin	2.3	3.3	0.05	0.05
Spleen	0.13	0.15	0.03	0.03
Pancreas	0.12	0.14	0.01	0.01
Blood	3.9	5.6	-	-

Table S2. Drug-related parameters used in the partition coefficient prediction methods and PBPK models.

Drug	logP	pK_a	fu_p	BP	fg	fa	K_a (1/h)	Cl_{hep} (L/h)	Cl_r (L/h)	Reference
Metoprolol	2.15	9.7	0.879	1.52	0.99	0.88	1.45	195	0	(Gaohua *et al.*, 2012)
Caffeine	-0.07	10.4	0.681	0.98	1	1	2.18	8	0.0383	(Gaohua *et al.*, 2012)
Voriconazole	2.56	1.76	0.42	1	-	-	0.849	14.075	0.096	(Zane and Thakker, 2014)
Alfentanil	2.2	6.5	0.11	0.63	-	-	0.849	38.88	0	(Björkman *et al.*, 1998)
Nevirapine	1.93	2.8	0.4	1.04	1	1	0.67	1.26	0.07	(De Sousa Mendes *et al.*, 2017)
Midazolam	3.1	6	0.059	1	0.59	0.88	3.04	1583	0	(Gaohua *et al.*, 2012)
Thiopental	2.9	7.5	0.13	1	-	-	0.849	13.8 (S), 17.7 (R)	0	(Nguyen *et al.*, 1996)
Nifedipine	2.2	3.93	0.04	0.73	0.73	1	1.91	938.5	0.07	(Ke *et al.*, 2012)
Digoxin	1.48	-	0.87	1	-	-	0.849	7.14	2.82	(Sumner and Russell, 1976)
Artemether	3.28	-	0.046	0.8	1	1	0.5	800	0	(Lin *et al.*, 2016)
Ofloxacin	-0.4	5.97 (acid), 9.28 (base)	0.77	0.92	-	-	0.849	8.92	2.76	(Flor *et al.*, 1993)

log*P* represents lipophilicity, fu_p is unbound fraction in plasma, BP is the blood:plasma ratio, fg is the gut bioavailability, fa is the fraction available for absorption from the dosage, K_a is the first-order absorption rate constant, Cl_{hep} is the hepatic clearance, and Cl_r is the renal clearance.

Table S3. Dosage information used in the partition coefficient prediction methods and PBPK models.

Drug	Dose	Route of administration	Rate	Inter-dose interval	Additional Doses	Reference
Metoprolol	10 mg	IV	-	-	-	(Gaohua *et al.*, 2012)
Caffeine	150 mg	PO	-	-	-	(Gaohua *et al.*, 2012)
Voriconazole	4 mg/kg	IV infusion	4 mg/kg/h	12 h	13	(Zane and Thakker, 2014)
Alfentanil	0.05 mg/kg	IV	-	-	-	(Björkman *et al.*, 1998)
Nevirapine	15 mg	IV	-	-	-	(De Sousa Mendes *et al.*, 2017)
Midazolam	2 mg	PO	-	-	-	(Gaohua *et al.*, 2012)
Thiopental	250 mg	IV	-	-	-	(Nguyen *et al.*, 1996)
Nifedipine	10 mg	PO	-	8 h	6	(Ke *et al.*, 2012)
Digoxin	0.013 mg	IV	-	-	-	(Sumner and Russell, 1976)
Artemether	80 mg	IV	-	8 h	1	(Lin *et al.*, 2016)
Ofloxacin	400 mg	IV infusion	400 mg/h	12 h	8	(Flor *et al.*, 1993)

Figure S1

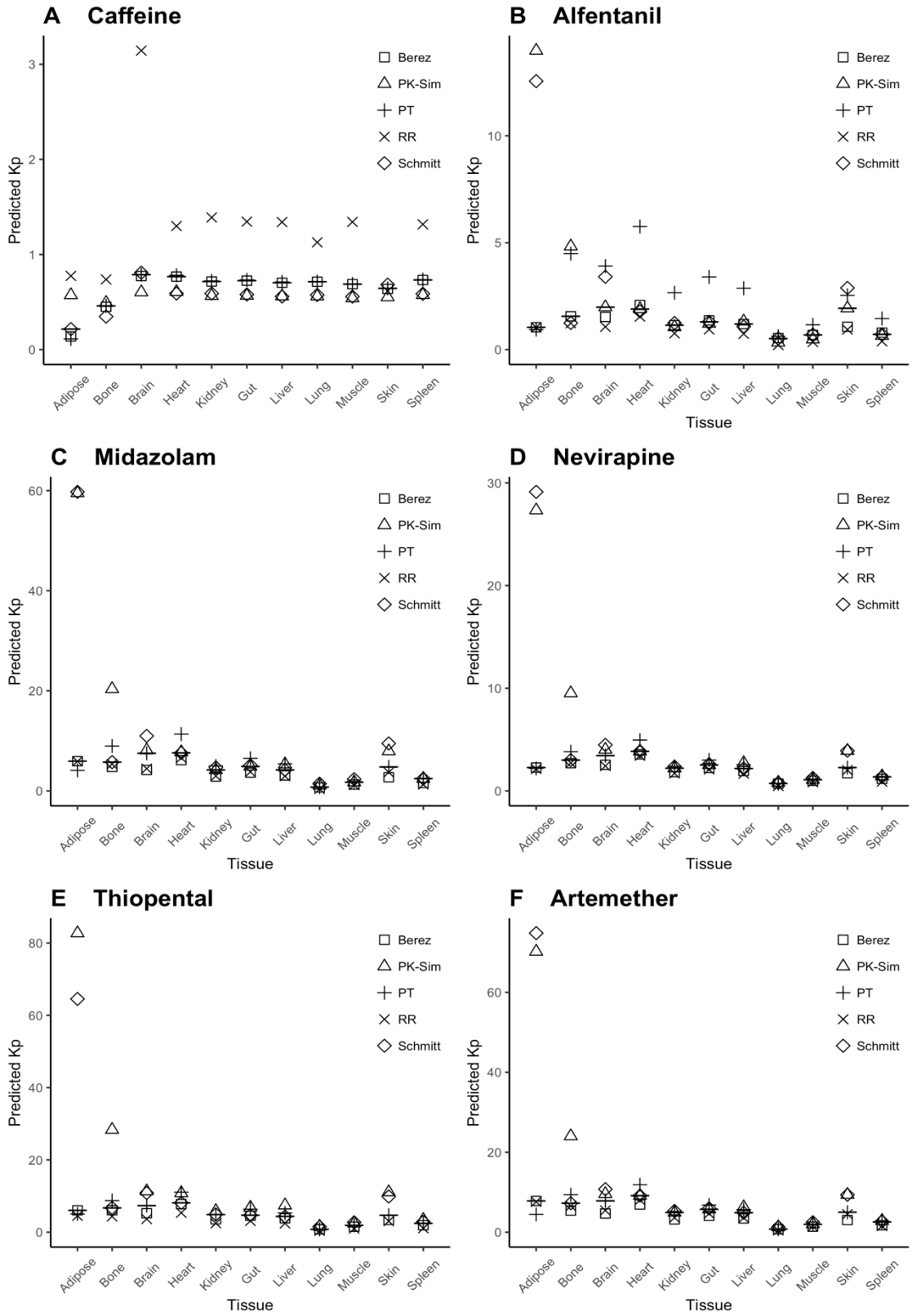
A Caffeine
B Alfentanil
C Midazolam
D Nevirapine
E Thiopental
F Artemether
Predicted Kp
Tissue
Adipose
Bone
Brain
Heart
Kidney
Gut
Liver
Lung
Muscle
Skin
Spleen
Berez
PK-Sim
PT
RR
Schmitt

Figure S1. Comparison of partition coefficient predictions for each method for additional drugs. The horizontal bars indicate the median partition coefficient for each tissue. (A-F) Partition coefficients for caffeine (strong base), alfentanil (weak base), midazolam (weak base), nevirapine (weak base), thiopental (acid), artemether (neutral).

Figure S2

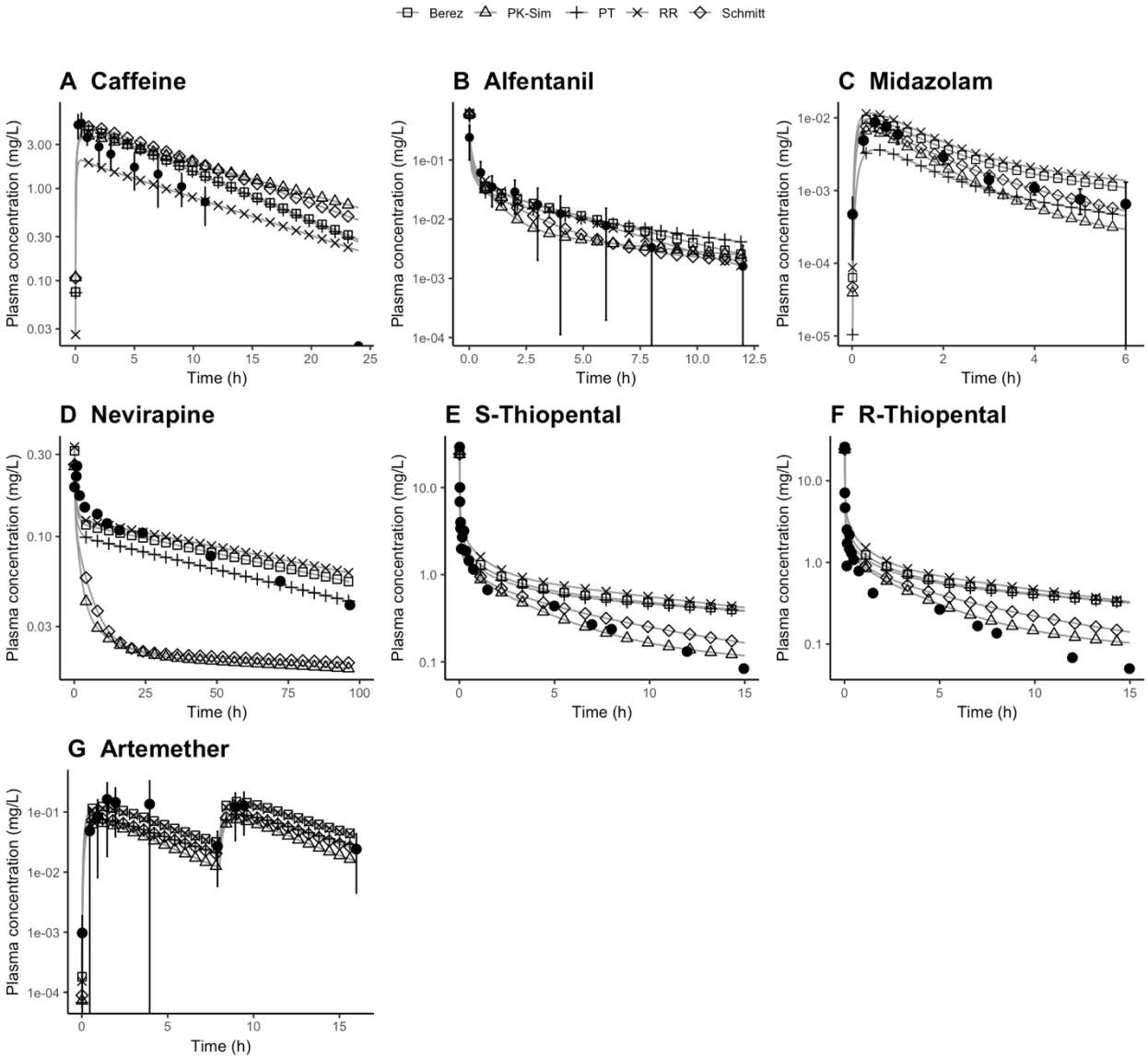

Figure S2. PBPK model predictions using each partition coefficient prediction method for additional drugs. Comparison between predictions for (A) caffeine (Gaohua *et al.*, 2012), (B) alfentanil (Björkman *et al.*, 1998), (C) midazolam (Gaohua *et al.*, 2012), (D) nevirapine (De Sousa Mendes *et al.*, 2017), (E) S-thiopental, (F) R-thiopental (Nguyen *et al.*, 1996) and (G) artemether (Lin *et al.*, 2016). Error bars represent standard deviations.

References

Björkman S, Wada DR, and Stanski DR (1998) Application of physiologic models to predict the influence of changes in body composition and blood flows on the pharmacokinetics of fentanyl and alfentanil in patients. *Anesthesiology* **88**:657–667.

De Sousa Mendes M, Lui G, Zheng Y, Pressiat C, Hirt D, Valade E, Bouazza N, Foissac F, Blanche S, Treluyer J-M, Urien S, and Benaboud S (2017) A Physiologically-Based Pharmacokinetic Model to Predict Human Fetal Exposure for a Drug Metabolized by Several CYP450 Pathways. *Clin Pharmacokinet* **56**:537–550.

Elmokadem A, Riggs MM, and Baron KT (2019) QSP and PBPK Modeling with mrgsolve: A Hands-on Tutorial. *CPT Pharmacometrics Syst Pharmacol*, doi: 10.1002/psp4.12467.

Flor SC, Rogge MC, and Chow AT (1993) Bioequivalence of oral and intravenous ofloxacin after multiple-dose administration to healthy male volunteers. *Antimicrob Agents Chemother* **37**:1468–1472.

Gaohua L, Abduljalil K, Jamei M, Johnson TN, and Rostami-Hodjegan A (2012) A pregnancy physiologically based pharmacokinetic (p-PBPK) model for disposition of drugs metabolized by CYP1A2, CYP2D6 and CYP3A4. *Br J Clin Pharmacol* **74**:873–885.

Ke AB, Nallani SC, Zhao P, Rostami-Hodjegan A, and Unadkat JD (2012) A PBPK Model to Predict Disposition of CYP3A-Metabolized Drugs in Pregnant Women: Verification and Discerning the Site of CYP3A Induction. *CPT Pharmacometrics Syst Pharmacol* **1**:e3.

Lin W, Heimbach T, Jain JP, Awasthi R, Hamed K, Sunkara G, and He H (2016) A Physiologically Based Pharmacokinetic Model to Describe Artemether Pharmacokinetics in Adult and Pediatric Patients. *J Pharm Sci* **105**:3205–3213.

Nguyen KT, Stephens DP, McLeish MJ, Crankshaw DP, and Morgan DJ (1996) Pharmacokinetics of thiopental and pentobarbital enantiomers after intravenous administration of racemic thiopental. *Anesth Analg* **83**:552–558.

Sumner DJ, and Russell AJ (1976) Digoxin pharmacokinetics: multicompartmental analysis and its clinical implications. *Br J Clin Pharmacol* **3**:221–229.

Valentin J (2002) Basic anatomical and physiological data for use in radiological protection: reference values. *Ann ICRP* **32**:1–277.

Zane NR, and Thakker DR (2014) A physiologically based pharmacokinetic model for voriconazole disposition predicts intestinal first-pass metabolism in children. *Clin Pharmacokinet* **53**:1171–1182.

Zhuang X, and Lu C (2016) PBPK modeling and simulation in drug research and development. *Acta Pharm Sin B* **6**:430–440.